

Quadrupole anisotropy in dihadron azimuthal correlations in central $d+Au$ collisions at $\sqrt{s_{NN}}=200$ GeV

A. Adare,¹³ C. Aidala,^{41,42} N.N. Ajitanand,⁵⁸ Y. Akiba,^{54,55} H. Al-Bataineh,⁴⁸ J. Alexander,⁵⁸ A. Angerami,¹⁴ K. Aoki,^{33,54} N. Apadula,⁵⁹ Y. Aramaki,^{12,54} E.T. Atomssa,³⁴ R. Averbeck,⁵⁹ T.C. Awes,⁵⁰ B. Azmoun,⁷ V. Babintsev,²³ M. Bai,⁶ G. Baksay,¹⁹ L. Baksay,¹⁹ K.N. Barish,⁸ B. Bassalleck,⁴⁷ A.T. Basye,¹ S. Bathe,^{5,8,55} V. Baublis,⁵³ C. Baumann,⁴³ A. Bazilevsky,⁷ S. Belikov,^{7,*} R. Belmont,⁶³ R. Bennett,⁵⁹ J.H. Bhom,⁶⁷ D.S. Blau,³² J.S. Bok,⁶⁷ K. Boyle,⁵⁹ M.L. Brooks,³⁷ H. Buesching,⁷ V. Bumazhnov,²³ G. Bunce,^{7,55} S. Butsyk,³⁷ S. Campbell,⁵⁹ A. Caringi,⁴⁴ C.-H. Chen,⁵⁹ C.Y. Chi,¹⁴ M. Chiu,⁷ I.J. Choi,⁶⁷ J.B. Choi,¹⁰ R.K. Choudhury,⁴ P. Christiansen,³⁹ T. Chujo,⁶² P. Chung,⁵⁸ O. Chvala,⁸ V. Cianciolo,⁵⁰ Z. Citron,⁵⁹ B.A. Cole,¹⁴ Z. Conesa del Valle,³⁴ M. Connors,⁵⁹ M. Csanád,¹⁷ T. Csörgő,⁶⁶ T. Dahms,⁵⁹ S. Dairaku,^{33,54} I. Danchev,⁶³ K. Das,²⁰ A. Datta,⁴¹ G. David,⁷ M.K. Dayananda,²¹ A. Denisov,²³ A. Deshpande,^{55,59} E.J. Desmond,⁷ K.V. Dharmawardane,⁴⁸ O. Dietzsch,⁵⁷ A. Dion,²⁷ M. Donadelli,⁵⁷ O. Drapier,³⁴ A. Drees,⁵⁹ K.A. Drees,⁶ J.M. Durham,⁵⁹ A. Durum,²³ D. Dutta,⁴ L. D'Orazio,⁴⁰ S. Edwards,²⁰ Y.V. Efremenko,⁵⁰ F. Ellinghaus,¹³ T. Engelmöore,¹⁴ A. Enokizono,⁵⁰ H. En'yo,^{54,55} S. Esumi,⁶² B. Fadern,⁴⁴ D.E. Fields,⁴⁷ M. Finger,⁹ M. Finger, Jr.,⁹ F. Fleuret,³⁴ S.L. Fokin,³² Z. Fraenkel,^{65,*} J.E. Frantz,^{49,59} A. Franz,⁷ A.D. Frawley,²⁰ K. Fujiwara,⁵⁴ Y. Fukao,⁵⁴ T. Fusayasu,⁴⁶ I. Garishvili,⁶⁰ A. Glenn,³⁶ H. Gong,⁵⁹ M. Gonin,³⁴ Y. Goto,^{54,55} R. Granier de Cassagnac,³⁴ N. Grau,^{2,14} S.V. Greene,⁶³ G. Grim,³⁷ M. Grosse Perdekamp,²⁴ T. Gunji,¹² H.-Å. Gustafsson,^{39,*} J.S. Haggerty,⁷ K.I. Hahn,¹⁸ H. Hamagaki,¹² J. Hamblen,⁶⁰ R. Han,⁵² J. Hanks,¹⁴ E. Haslum,³⁹ R. Hayano,¹² X. He,²¹ M. Heffner,³⁶ T.K. Hemmick,⁵⁹ T. Hester,⁸ J.C. Hill,²⁷ M. Hohlmann,¹⁹ W. Holzmann,¹⁴ K. Homma,²² B. Hong,³¹ T. Horaguchi,²² D. Hornback,⁶⁰ S. Huang,⁶³ T. Ichihara,^{54,55} R. Ichimiya,⁵⁴ Y. Ikeda,⁶² K. Imai,^{28,33,54} M. Inaba,⁶² D. Isenhower,¹ M. Ishihara,⁵⁴ M. Issah,⁶³ D. Ivanishev,⁵³ Y. Iwanaga,²² B.V. Jacak,⁵⁹ J. Jia,^{7,58} X. Jiang,³⁷ J. Jin,¹⁴ B.M. Johnson,⁷ T. Jones,¹ K.S. Joo,⁴⁵ D. Jouan,⁵¹ D.S. Jumper,¹ F. Kajihara,¹² J. Kamin,⁵⁹ J.H. Kang,⁶⁷ J. Kapustinsky,³⁷ K. Karatsu,^{33,54} M. Kasai,^{54,56} D. Kawall,^{41,55} M. Kawashima,^{54,56} A.V. Kazantsev,³² T. Kempel,²⁷ A. Khanzadeev,⁵³ K.M. Kijima,²² J. Kikuchi,⁶⁴ A. Kim,¹⁸ B.I. Kim,³¹ D.J. Kim,²⁹ E.-J. Kim,¹⁰ Y.-J. Kim,²⁴ E. Kinney,¹³ Á. Kiss,¹⁷ E. Kistenev,⁷ D. Kleinjan,⁸ L. Kochenda,⁵³ B. Komkov,⁵³ M. Konno,⁶² J. Koster,²⁴ A. Král,¹⁵ A. Kravitz,¹⁴ G.J. Kunde,³⁷ K. Kurita,^{54,56} M. Kurosawa,⁵⁴ Y. Kwon,⁶⁷ G.S. Kyle,⁴⁸ R. Lacey,⁵⁸ Y.S. Lai,¹⁴ J.G. Lajoie,²⁷ A. Lebedev,²⁷ D.M. Lee,³⁷ J. Lee,¹⁸ K.B. Lee,³¹ K.S. Lee,³¹ M.J. Leitch,³⁷ M.A.L. Leite,⁵⁷ X. Li,¹¹ P. Lichtenwalner,⁴⁴ P. Liebing,⁵⁵ L.A. Linden Levy,¹³ T. Liška,¹⁵ H. Liu,³⁷ M.X. Liu,³⁷ B. Love,⁶³ D. Lynch,⁷ C.F. Maguire,⁶³ Y.I. Makdisi,⁶ M.D. Malik,⁴⁷ V.I. Manko,³² E. Mannel,¹⁴ Y. Mao,^{52,54} H. Masui,⁶² F. Matathias,¹⁴ M. McCumber,⁵⁹ P.L. McGaughey,³⁷ D. McGlinchey,^{13,20} N. Means,⁵⁹ B. Meredith,²⁴ Y. Miake,⁶² T. Mibe,³⁰ A.C. Mignerey,⁴⁰ K. Miki,^{54,62} A. Milov,⁷ J.T. Mitchell,⁷ A.K. Mohanty,⁴ H.J. Moon,⁴⁵ Y. Morino,¹² A. Morreale,⁸ D.P. Morrison,^{7,†} T.V. Moukhanova,³² T. Murakami,³³ J. Murata,^{54,56} S. Nagamiya,³⁰ J.L. Nagle,^{13,‡} M. Naglis,⁶⁵ M.I. Nagy,⁶⁶ I. Nakagawa,^{54,55} Y. Nakamiya,²² K.R. Nakamura,^{33,54} T. Nakamura,⁵⁴ K. Nakano,⁵⁴ S. Nam,¹⁸ J. Newby,³⁶ M. Nguyen,⁵⁹ M. Nihashi,²² R. Nouicer,⁷ A.S. Nyanin,³² C. Oakley,²¹ E. O'Brien,⁷ S.X. Oda,¹² C.A. Ogilvie,²⁷ M. Oka,⁶² K. Okada,⁵⁵ Y. Onuki,⁵⁴ A. Oskarsson,³⁹ M. Ouchida,^{22,54} K. Ozawa,¹² R. Pak,⁷ V. Pantuev,^{25,59} V. Papavassiliou,⁴⁸ I.H. Park,¹⁸ S.K. Park,³¹ W.J. Park,³¹ S.F. Pate,⁴⁸ H. Pei,²⁷ J.-C. Peng,²⁴ H. Pereira,¹⁶ D. Perepelitsa,¹⁴ D.Yu. Peressounko,³² R. Petti,⁵⁹ C. Pinkenburg,⁷ R.P. Pisani,⁷ M. Proissl,⁵⁹ M.L. Purschke,⁷ H. Qu,²¹ J. Rak,²⁹ I. Ravinovich,⁶⁵ K.F. Read,^{50,60} S. Rembeczki,¹⁹ K. Reygers,⁴³ V. Riabov,⁵³ Y. Riabov,⁵³ E. Richardson,⁴⁰ D. Roach,⁶³ G. Roche,³⁸ S.D. Rolnick,⁸ M. Rosati,²⁷ C.A. Rosen,¹³ S.S.E. Rosendahl,³⁹ P. Ružička,²⁶ B. Sahlmueller,^{43,59} N. Saito,³⁰ T. Sakaguchi,⁷ K. Sakashita,^{54,61} V. Samsonov,⁵³ S. Sano,^{12,64} T. Sato,⁶² S. Sawada,³⁰ K. Sedgwick,⁸ J. Seele,¹³ R. Seidl,^{24,55} R. Seto,⁸ D. Sharma,⁶⁵ I. Shein,²³ T.-A. Shibata,^{54,61} K. Shigaki,²² M. Shimomura,⁶² K. Shoji,^{33,54} P. Shukla,⁴ A. Sickles,⁷ C.L. Silva,²⁷ D. Silvermyr,⁵⁰ C. Silvestre,¹⁶ K.S. Sim,³¹ B.K. Singh,³ C.P. Singh,³ V. Singh,³ M. Slunečka,⁹ R.A. Soltz,³⁶ W.E. Sondheim,³⁷ S.P. Sorensen,⁶⁰ I.V. Sourikova,⁷ P.W. Stankus,⁵⁰ E. Stenlund,³⁹ S.P. Stoll,⁷ T. Sugitate,²² A. Sukhanov,⁷ J. Sziklai,⁶⁶ E.M. Takagui,⁵⁷ A. Taketani,^{54,55} R. Tanabe,⁶² Y. Tanaka,⁴⁶ S. Taneja,⁵⁹ K. Tanida,^{33,54,55} M.J. Tannenbaum,⁷ S. Tarafdar,³ A. Taranenko,⁵⁸ H. Themann,⁵⁹ D. Thomas,¹ T.L. Thomas,⁴⁷ M. Togawa,⁵⁵ A. Toia,⁵⁹ L. Tomášek,²⁶ H. Torii,²² R.S. Towell,¹ I. Tserruya,⁶⁵ Y. Tsuchimoto,²² C. Vale,⁷ H. Valle,⁶³ H.W. van Hecke,³⁷ E. Vazquez-Zambrano,¹⁴ A. Veicht,²⁴ J. Velkovska,⁶³ R. Vértesi,⁶⁶ M. Virius,¹⁵ V. Vrba,²⁶ E. Vznuzdaev,⁵³ X.R. Wang,⁴⁸ D. Watanabe,²² K. Watanabe,⁶² Y. Watanabe,^{54,55} F. Wei,²⁷ R. Wei,⁵⁸ J. Wessels,⁴³ S.N. White,⁷ D. Winter,¹⁴ C.L. Woody,⁷

R.M. Wright,¹ M. Wysocki,¹³ Y.L. Yamaguchi,¹² K. Yamaura,²² R. Yang,²⁴ A. Yanovich,²³ J. Ying,²¹
S. Yokkaichi,^{54,55} Z. You,⁵² G.R. Young,⁵⁰ I. Younus,^{35,47} I.E. Yushmanov,³² W.A. Zajc,¹⁴ and S. Zhou¹¹

(PHENIX Collaboration)

- ¹Abilene Christian University, Abilene, Texas 79699, USA
²Department of Physics, Augustana College, Sioux Falls, South Dakota 57197, USA
³Department of Physics, Banaras Hindu University, Varanasi 221005, India
⁴Bhabha Atomic Research Centre, Bombay 400 085, India
⁵Baruch College, City University of New York, New York, New York, 10010 USA
⁶Collider-Accelerator Department, Brookhaven National Laboratory, Upton, New York 11973-5000, USA
⁷Physics Department, Brookhaven National Laboratory, Upton, New York 11973-5000, USA
⁸University of California - Riverside, Riverside, California 92521, USA
⁹Charles University, Ovocný trh 5, Praha 1, 116 36, Prague, Czech Republic
¹⁰Chonbuk National University, Jeonju, 561-756, Korea
¹¹Science and Technology on Nuclear Data Laboratory, China Institute of Atomic Energy, Beijing 102413, P. R. China
¹²Center for Nuclear Study, Graduate School of Science, University of Tokyo, 7-3-1 Hongo, Bunkyo, Tokyo 113-0033, Japan
¹³University of Colorado, Boulder, Colorado 80309, USA
¹⁴Columbia University, New York, New York 10027 and Nevis Laboratories, Irvington, New York 10533, USA
¹⁵Czech Technical University, Zikova 4, 166 36 Prague 6, Czech Republic
¹⁶Dapnia, CEA Saclay, F-91191, Gif-sur-Yvette, France
¹⁷ELTE, Eötvös Loránd University, H - 1117 Budapest, Pázmány P. s. 1/A, Hungary
¹⁸Ewha Womans University, Seoul 120-750, Korea
¹⁹Florida Institute of Technology, Melbourne, Florida 32901, USA
²⁰Florida State University, Tallahassee, Florida 32306, USA
²¹Georgia State University, Atlanta, Georgia 30303, USA
²²Hiroshima University, Kagamiyama, Higashi-Hiroshima 739-8526, Japan
²³IHEP Protvino, State Research Center of Russian Federation, Institute for High Energy Physics, Protvino, 142281, Russia
²⁴University of Illinois at Urbana-Champaign, Urbana, Illinois 61801, USA
²⁵Institute for Nuclear Research of the Russian Academy of Sciences, prospekt 60-letiya Oktyabrya 7a, Moscow 117312, Russia
²⁶Institute of Physics, Academy of Sciences of the Czech Republic, Na Slovance 2, 182 21 Prague 8, Czech Republic
²⁷Iowa State University, Ames, Iowa 50011, USA
²⁸Advanced Science Research Center, Japan Atomic Energy Agency, 2-4
Shirakata Shirane, Tokai-mura, Naka-gun, Ibaraki-ken 319-1195, Japan
²⁹Helsinki Institute of Physics and University of Jyväskylä, P.O.Box 35, FI-40014 Jyväskylä, Finland
³⁰KEK, High Energy Accelerator Research Organization, Tsukuba, Ibaraki 305-0801, Japan
³¹Korea University, Seoul, 136-701, Korea
³²Russian Research Center "Kurchatov Institute", Moscow, 123098 Russia
³³Kyoto University, Kyoto 606-8502, Japan
³⁴Laboratoire Leprince-Ringuet, Ecole Polytechnique, CNRS-IN2P3, Route de Saclay, F-91128, Palaiseau, France
³⁵Physics Department, Lahore University of Management Sciences, Lahore, Pakistan
³⁶Lawrence Livermore National Laboratory, Livermore, California 94550, USA
³⁷Los Alamos National Laboratory, Los Alamos, New Mexico 87545, USA
³⁸LPC, Université Blaise Pascal, CNRS-IN2P3, Clermont-Fd, 63177 Aubiere Cedex, France
³⁹Department of Physics, Lund University, Box 118, SE-221 00 Lund, Sweden
⁴⁰University of Maryland, College Park, Maryland 20742, USA
⁴¹Department of Physics, University of Massachusetts, Amherst, Massachusetts 01003-9337, USA
⁴²Department of Physics, University of Michigan, Ann Arbor, Michigan 48109-1040, USA
⁴³Institut für Kernphysik, University of Muenster, D-48149 Muenster, Germany
⁴⁴Muhlenberg College, Allentown, Pennsylvania 18104-5586, USA
⁴⁵Myongji University, Yongin, Kyonggido 449-728, Korea
⁴⁶Nagasaki Institute of Applied Science, Nagasaki-shi, Nagasaki 851-0193, Japan
⁴⁷University of New Mexico, Albuquerque, New Mexico 87131, USA
⁴⁸New Mexico State University, Las Cruces, New Mexico 88003, USA
⁴⁹Department of Physics and Astronomy, Ohio University, Athens, Ohio 45701, USA
⁵⁰Oak Ridge National Laboratory, Oak Ridge, Tennessee 37831, USA
⁵¹IPN-Orsay, Université Paris Sud, CNRS-IN2P3, BP1, F-91406, Orsay, France
⁵²Peking University, Beijing 100871, P. R. China
⁵³PNPI, Petersburg Nuclear Physics Institute, Gatchina, Leningrad region, 188300, Russia
⁵⁴RIKEN Nishina Center for Accelerator-Based Science, Wako, Saitama 351-0198, Japan
⁵⁵RIKEN BNL Research Center, Brookhaven National Laboratory, Upton, New York 11973-5000, USA
⁵⁶Physics Department, Rikkyo University, 3-34-1 Nishi-Ikebukuro, Toshima, Tokyo 171-8501, Japan
⁵⁷Universidade de São Paulo, Instituto de Física, Caixa Postal 66318, São Paulo CEP05315-970, Brazil
⁵⁸Chemistry Department, Stony Brook University, SUNY, Stony Brook, New York 11794-3400, USA
⁵⁹Department of Physics and Astronomy, Stony Brook University, SUNY, Stony Brook, New York 11794-3400, USA

⁶⁰University of Tennessee, Knoxville, Tennessee 37996, USA

⁶¹Department of Physics, Tokyo Institute of Technology, Oh-okayama, Meguro, Tokyo 152-8551, Japan

⁶²Institute of Physics, University of Tsukuba, Tsukuba, Ibaraki 305, Japan

⁶³Vanderbilt University, Nashville, Tennessee 37235, USA

⁶⁴Waseda University, Advanced Research Institute for Science and Engineering, 17 Kikui-cho, Shinjuku-ku, Tokyo 162-0044, Japan

⁶⁵Weizmann Institute, Rehovot 76100, Israel

⁶⁶Institute for Particle and Nuclear Physics, Wigner Research Centre for Physics, Hungarian Academy of Sciences (Wigner RCP, RMKI) H-1525 Budapest 114, POBox 49, Budapest, Hungary

⁶⁷Yonsei University, IPAP, Seoul 120-749, Korea

(Dated: September 11, 2018)

The PHENIX collaboration at the Relativistic Heavy Ion Collider (RHIC) reports measurements of azimuthal dihadron correlations near midrapidity in d +Au collisions at $\sqrt{s_{NN}}=200$ GeV. These measurements complement recent analyses by experiments at the Large Hadron Collider (LHC) involving central p +Pb collisions at $\sqrt{s_{NN}}=5.02$ TeV, which have indicated strong anisotropic long-range correlations in angular distributions of hadron pairs. The origin of these anisotropies is currently unknown. Various competing explanations include parton saturation and hydrodynamic flow. We observe qualitatively similar anisotropies at RHIC to those seen at the LHC, and when both are divided by an estimate of the initial-state eccentricity, the anisotropies follow a common multiplicity scaling. This scaling is also found to extend to heavy ion data at RHIC and the LHC, where the anisotropies are widely thought to be due to hydrodynamic flow. The results presented here, at much lower collision energy and with a deuteron projectile (instead of a proton), provide important new information for understanding the origin of these new long-range correlations.

PACS numbers: 25.75.Dw

Proton- and deuteron-nucleus collisions at relativistic energies have been studied in order to provide baseline measurements for heavy ion collisions. In $p(d)$ +A collisions, initial-state nuclear effects are present; however, the formation of hot quark-gluon matter as created in heavy ion collisions is not commonly expected. Recently there has been significant interest in the physics of very high multiplicity events in small collision systems, motivated by the observation of a small azimuthal angle ($\Delta\phi$) large pseudorapidity ($\Delta\eta$) correlation of primarily low p_T particles in very high multiplicity p + p collisions at 7 TeV [1]. The correlation strikingly resembles the “near-side ridge” observed in Au+Au at 200 GeV [2, 3]. The initial p + p result sparked considerable theoretical interest [4–6]. Recently, a similar effect was observed in p +Pb collisions at $\sqrt{s_{NN}} = 5.02$ TeV [7]. Subsequent work removed centrality independent correlations (largely from jet fragmentation) by looking at the difference in correlations between central and peripheral events and has additionally uncovered similar long-range $\Delta\eta$ correlations on the opposite side ($\Delta\phi \approx \pi$) beyond those expected from fragmentation of recoiling jets measured by ALICE [8] and ATLAS [9]. The effect appears as a longitudinally-extended azimuthal modulation with a predominantly quadrupole component (i.e. $\cos 2\Delta\phi$) and bears a qualitative resemblance in both magnitude and p_T dependence to elliptic flow measurements in heavy ion collisions, where the large quadrupole modulation is understood to be caused by the initial-state spatial anisotropy followed by a nearly inviscid hydrodynamic expansion [10]. A variety of physical mechanisms have been invoked to explain the observed anisotropies in p +Pb including gluon satu-

ration [6, 11–13], hydrodynamics [5, 14, 15], multiparton interactions [16], and final-state expansion effects [17].

Previous analyses involving two-particle correlations from d +Au collisions at RHIC have not indicated any long-range features at small $\Delta\phi$ [2, 18–20]. However, these measurements involved p_T selections which emphasize jet-like correlations, rather than the underlying event. Also, Refs. [19, 20] were based on d +Au collisions recorded in 2003 with a small data sample which limited the statistical significance of the results.

We present here the first analysis of very central d +Au events to measure hadron correlations between midrapidity particles at $\sqrt{s_{NN}} = 200$ GeV. The center of mass energy per nucleon is a factor of 25 lower than at the LHC, and another potentially key difference is the use of a deuteron as the projectile nucleus rather than a proton. In Ref. [14], within the context of a Monte Carlo Glauber model, the calculated initial spatial eccentricity of the participating nucleons, ε_2 , for central (large number of participants) d +Pb is more than a factor of two larger than in central p +Pb collisions at LHC energies. We find the initial spatial eccentricity ε_2 from Monte Carlo Glauber [21] for d +Au at RHIC energies to be similar to the d +Pb calculations at LHC energies.

The results presented here are based on 1.56 billion minimum-bias d +Au collisions at $\sqrt{s_{NN}} = 200$ GeV recorded with the PHENIX detector in 2008. The event centrality in d +Au is determined by categorizing the integrated charge by upper percentile as seen by a beam-beam counter (BBC) facing the incoming Au nucleus [22]. Here we isolate a more central sample than previously analyzed, in order to compare more closely to the LHC

results. We use central and peripheral event samples comprising the top 5% and 50–88% of the total charge distributions, respectively.

This analysis considers charged hadrons measured within the two PHENIX central arm spectrometers. Each arm covers nominally $\pi/2$ in azimuth and has a pseudorapidity acceptance of $|\eta| < 0.35$. Charged tracks are reconstructed using the drift chambers with a hit association requirement in two layers of multiwire proportional chambers with pad readout, achieving a momentum resolution of $0.7\% \oplus 1.1\%p$ (GeV/c). Only tracks with full and unambiguous drift-chamber and pad-chamber-1 hit information are used. Electrons are rejected with a veto in the ring-imaging Čerenkov (RICH) counters.

All pairs satisfying the tracking cuts within an event are measured. The measured pairs are then corrected for the PHENIX azimuthal acceptance through use of mixed event distributions. The conditional yield of pairs is determined by:

$$\frac{1}{N^t} \frac{dN^{\text{pairs}}}{d\Delta\phi} \propto \frac{dN^{\text{pairs}}_{\text{same}}/d\Delta\phi}{dN^{\text{pairs}}_{\text{mix}}/d\Delta\phi} \quad (1)$$

where N^t is the number of *trigger* hadrons (trigger hadrons are those which have the momenta required to begin the search for a pair of hadrons) and $N^{\text{pairs}}_{\text{same}}$ ($N^{\text{pairs}}_{\text{mix}}$) is the number of pairs from the same (mixed) events. Mixed pairs are constructed with particles from different events within the same 5% centrality class and with event vertices within 5 cm of each other. Since the focus of this analysis is on the shape of the distributions, no correction is applied for the track reconstruction efficiency, which has a negligible dependence on centrality for d +Au track multiplicities.

In order to make direct comparisons between our measurements and recent ATLAS p +Pb results [9], we follow a similar analysis procedure. Charged hadron selections are made at different momenta from 0.5 through 3.5 GeV/c. For this analysis, each pair includes at least one particle at low p_T ($0.5 < p_T < 0.75$ GeV/c) in order to enhance the sensitivity to the nonjet phenomena. The pairs are restricted to pseudorapidity separations of $0.48 < |\Delta\eta| < 0.7$, in order to minimize the contribution from small-angle correlations arising from resonances, Bose-Einstein correlations, and jet fragmentation. This pseudorapidity gap is chosen to be as large as possible within the PHENIX tracking acceptance, while still preserving an adequate statistical sample size.

The associated yield due to azimuthally uncorrelated background is estimated by means of the zero-yield-at-minimum (ZYAM) procedure [23]. This background contribution is obtained for both the central and peripheral samples by performing fits to the conditional yields using a functional form composed of a constant pedestal and two Gaussian peaks, centered at $\Delta\phi = 0$ and π . The

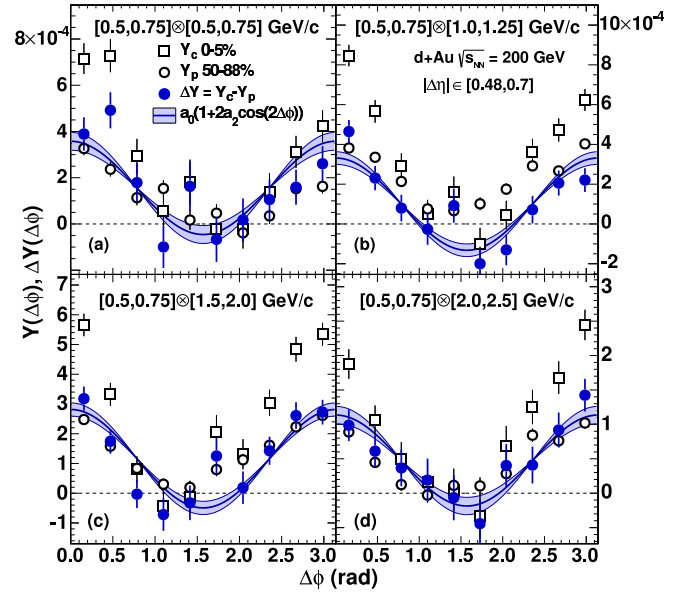


FIG. 1: (color online) Azimuthal conditional yields, $Y(\Delta\phi)$, for (open [black] squares) 0–5% most central and (open [black] circles) peripheral (50–88% least central) collisions with a minimum $\Delta\eta$ separation of 0.48 units. (filled [blue] circles) Difference $\Delta Y(\Delta\phi)$, which is $(Y_c - Y_p)$ (blue curve) fit to $a_0 + 2a_2 \cos(2\Delta\phi)$, where a_0 and a_2 are computed directly from the data. (shaded [blue] band) Statistical uncertainty on a_2 . No correction for the $\Delta\phi$ independent reconstruction efficiency has been applied.

minimum of this function, b_{ZYAM} , is subtracted from the $\Delta\phi$ distributions, and the result is $Y(\Delta\phi)$:

$$Y(\Delta\phi) \equiv \frac{1}{N^t} \frac{dN^{\text{pairs}}}{d\Delta\phi} - b_{\text{ZYAM}} \quad (2)$$

The conditional yields $Y_c(\Delta\phi)$ and $Y_p(\Delta\phi)$ (central and peripheral events, respectively) are shown in Fig. 1, along with their difference $\Delta Y(\Delta\phi) \equiv Y_c(\Delta\phi) - Y_p(\Delta\phi)$. As in Ref. [9], this subtraction removes any centrality independent correlations, such as effects from unmodified jet fragmentation, resonances and HBT. In the absence of any centrality dependence, $Y_c(\Delta\phi)$ and $Y_p(\Delta\phi)$ should be identical. Due to the limitations of our method, any signal in the peripheral events is subtracted from the central events. We see that $Y_c(\Delta\phi)$ is significantly larger than $Y_p(\Delta\phi)$ for $\Delta\phi$ near 0 and π .

In a manner similar to Ref. [9], we find that the difference with centrality is well described by the symmetric form: $\Delta Y(\Delta\phi) \approx a_0 + 2a_2 \cos(2\Delta\phi)$ as demonstrated in Fig. 1. The coefficients a_n and their statistical uncertainties are computed from the $\Delta Y(\Delta\phi)$ distributions as: $a_n = \langle \Delta Y(\Delta\phi) \cos(n\Delta\phi) \rangle$. The $\cos(2\Delta\phi)$ modulation appears as the dominant component of the anisotropy for all trigger/partner combinations as will be quantified below.

The PHENIX central arm spectrometers lack sufficient $|\Delta\eta|$ acceptance to completely exclude the near-side jet

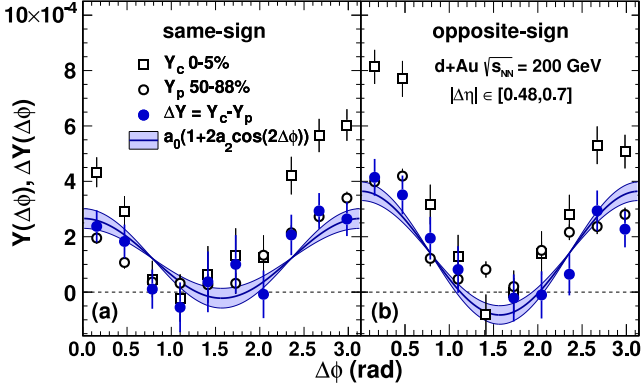


FIG. 2: (color online) Sample comparison of $Y(\Delta\phi)$ and $\Delta Y(\Delta\phi)$ for same and oppositely charged pairs for $1.25 < p_T^a < 1.5$ GeV/c and $0.48 < |\Delta\eta| < 0.7$. The symbols, curve, and shaded band are as described in the Fig. 1 caption.

peak. To assess the systematic influence of any residual unmodified jet correlations, we analyzed charge-selected correlations. Charge-ordering is a known feature of jet fragmentation which leads to enhancement of the jet correlation in opposite-sign pairs, and suppression in like-sign pairs, in the near side peak (e.g. Ref. [24]). A representative p_T selection of $Y(\Delta\phi)$ and $\Delta Y(\Delta\phi)$ distributions are shown in Fig. 2, where all charge combinations exhibit a significant $\cos 2\Delta\phi$ modulation. The magnitude of the modulation is larger in the opposite-sign case, indicating some residual unmodified jet correlation contribution. We also varied the $|\Delta\eta|$ window which changes the residual jet contribution. Both of these cross-checks are used to estimate the systematic uncertainty, as discussed later.

In order to quantify the relative amplitude of the azimuthal modulation we define $c_n \equiv a_n / (b_{ZYAM}^c + a_0)$ where b_{ZYAM}^c is b_{ZYAM} in central events. This quantity is shown as a function of associated p_T in Fig. 3 for central (0–5%) collisions.

The centrality dependence will be analyzed in further detail in a forthcoming publication, though we note that we have observed a signal of similar magnitude for the 0–20% most central collisions. The ATLAS c_2 results [9] have a qualitatively similar p_T^a dependence, but with a significantly smaller magnitude. However, it must be noted that the c_2 values from PHENIX and ATLAS are not directly comparable since c_2 is a function of the p_T of both particles and the trigger particle p_T range is not identical in the two analyses. ATLAS has also used a much larger $\Delta\eta$ separation between the particles.

The c_3 values, shown in Fig. 3, are small relative to c_2 . Fitting the c_3 data to a constant yields $(6 \pm 4) \times 10^{-4}$ with a χ^2/dof of 8.4/7 (statistical uncertainties only). The current precision is inadequate to reveal the existence of a significant c_3 signal.

In p +Pb collisions the signal is seen in long range $\Delta\eta$

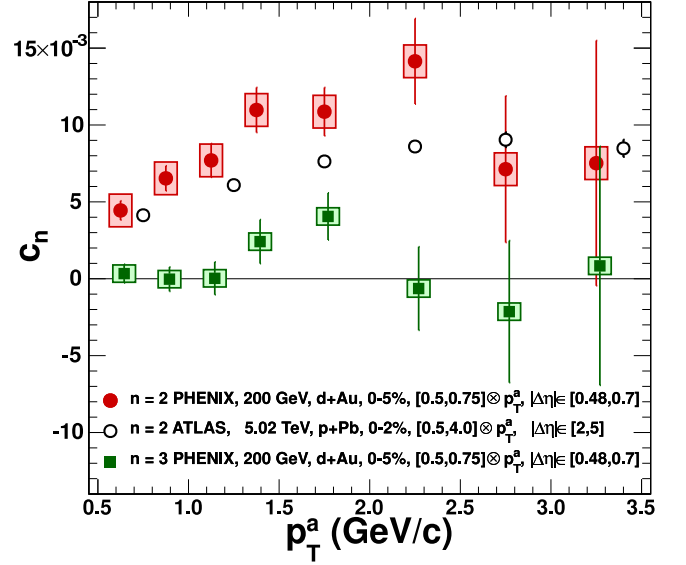


FIG. 3: (color online) The n th-order pair anisotropy, c_n , of the central collision excess as a function of associated particle p_T^a . PHENIX (filled [red] circles) c_2 and (open [black] circles) c_3 are for $0.5 < p_T^t < 0.75$ GeV/c, $0.48 < |\Delta\eta| < 0.7$ and ATLAS (filled [green] squares) c_2 [9] are for $0.5 < p_T^t < 4.0$ GeV/c, $2 < |\Delta\eta| < 5$.

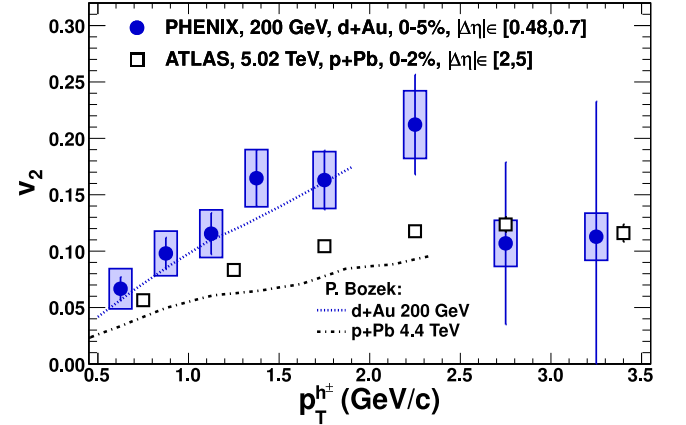


FIG. 4: (color online) Charged hadron second-order anisotropy, v_2 , as a function transverse momentum for (filled [blue] circles) PHENIX and (open [black] circles) ATLAS [9]. Also shown are a hydrodynamic calculation [14, 25] for (upper [blue] curve) d +Au collisions at $\sqrt{s_{NN}} = 200$ GeV and (lower [black] curve) 0–4% central p +Pb collisions at $\sqrt{s_{NN}} = 4.4$ TeV.

correlations. Here, signal is measured at midrapidity, but it is natural to ask if previous PHENIX rapidity separated correlation measurements [18] would have been sensitive to a signal of this magnitude, if it is present. The maximum c_2 observed here is approximately a 1% modulation about the background level. Overlaying a modulation of this size on the conditional yields shown in Fig. 1 of Ref. [18] shows that the modulation on the near

side is small compared with the statistical uncertainties on the points. In the current analysis, both particles are near midrapidity, while the analysis in Ref [18] includes one of the particles very forward ($3.0 < \eta < 3.8$) in the d -going direction. Thus, with the current results we cannot determine whether the signal observed here persists for $\eta > 3$.

A measure of the single-particle anisotropy, v_2 , can be obtained under the assumption of factorization [26–28], which gives the relation $c_2(p_T^t, p_T^a) = v_2(p_T^t) \times v_2(p_T^a)$. We have varied p_T^t and recomputed $v_2(p_T)$ and find no significant deviation from this factorization hypothesis. The calculated single particle v_2 is shown in Fig. 4, and also compared with the ATLAS [9] results, again revealing qualitatively similar p_T dependence with a significantly larger magnitude. We also compare the v_2 results to a hydrodynamic calculation [14, 25] and find good agreement between the data and the calculation, which predicts larger anisotropy in d +Au than p +Pb collisions (the calculation for p +Pb is for 0–4% centrality at 4.4 TeV, not 0–2% central at 5.02 TeV as in the data).

The systematic uncertainties as shown in Figs. 3 and 4 are estimated as the root-mean-squared variation of the same-sign and opposite-sign c_n measurements about the combined value to reflect the influence of possible remaining jet correlations. This systematic uncertainty is applied symmetrically, since the influence of the jet contribution is not known. As a test, the $\Delta\eta$ interval was varied from the nominal value of 0.48 to 0.36 and 0.60. The c_n values remained unchanged within statistical uncertainties, with the qualification that the $|\Delta\eta| > 0.6$ sample lacks sufficient statistics for a precise comparison at higher p_T . We also produced v_2 values with different trigger particle momentum selections and found no significant change in the extracted values. Other sources of uncertainty, such as occupancy and acceptance corrections, were also found to have negligible effect on these results.

In order to further investigate the origin of this effect in Fig. 5 we plot the RHIC and LHC results scaled by ε_2 as calculated in a Glauber Monte Carlo as a function of the charged particle multiplicity at midrapidity. The 0–5% d +Au collisions at $\sqrt{s_{NN}} = 200$ GeV have a $dN_{ch}/d\eta$ similar to those of midcentral p +Pb collisions at the LHC, while the ε_2 values for d +Au collisions are about 50% larger than those calculated for the midcentral p +Pb collisions. The key observation is that the ratio v_2/ε_2 is consistent between RHIC and the LHC, despite the factor of 25 difference in collision center of mass energy. A continuation of this same trend is seen by also comparing to v_2/ε_2 as measured in Au+Au [30–32] and Pb+Pb [33, 34] collisions.

In summary, a two-particle anisotropy at midrapidity in the 5% most central d +Au collisions at $\sqrt{s_{NN}} = 200$ GeV is observed. The excess yield in central compared to peripheral events is well described by

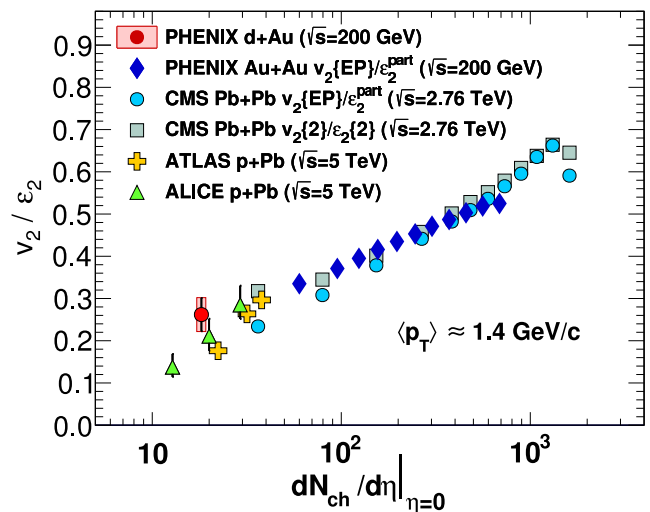


FIG. 5: (color online) The eccentricity-scaled anisotropy, v_2/ε_2 , vs charged-particle multiplicity ($dN_{ch}/d\eta$) for $p(d)$ +A collisions measured by PHENIX, ATLAS [9], and ALICE [8]. Also shown are Au+Au data at $\sqrt{s_{NN}} = 200$ GeV [30–32] and Pb+Pb data at $\sqrt{s_{NN}} = 2.76$ TeV [33, 34]. The v_2 are for similar p_T selections. Due to the lack of available multiplicity data in p +Pb and d +Au collisions the $dN_{ch}/d\eta$ values for those systems are calculated from HIJING [29].

a quadrupole shape. The signal is qualitatively similar to that observed in long range correlations observed in p +Pb collisions at much higher energies, but with a significantly larger amplitude than that observed in 0–2% central p +Pb collisions at ATLAS. While our acceptance does not allow us to exclude the possibility of centrality dependent modifications to the jet correlations, the subtraction of the peripheral jet like correlations has been checked both by varying the $\Delta\eta$ cuts and exploiting the charge sign dependence of jet-induced correlations. The observed results are in agreement with a hydrodynamic calculation for d +Au collisions at $\sqrt{s_{NN}} = 200$ GeV.

We find that scaling the results from RHIC and the LHC by the initial second order participant eccentricity brings the RHIC and LHC results to a common curve as a function of $dN_{ch}/d\eta$ also shared by elliptic flow coefficients from Au+Au and Pb+Pb collisions. This finding suggests that these phenomena are sensitive to the initial state geometry and that the same underlying mechanism is responsible in both p +Pb collisions at the LHC and d +Au collisions at RHIC. It also suggests a relationship to the hydrodynamic understanding of v_2 in heavy ion collisions. The observation of these correlations at both RHIC and the LHC provides important new information for understanding these phenomena. Models which seek to describe these features must be capable of also explaining their persistence as the center of mass energy is varied by a factor of 25.

We thank the staff of the Collider-Accelerator and Physics Departments at Brookhaven National Labora-

tory and the staff of the other PHENIX participating institutions for their vital contributions. We acknowledge support from the Office of Nuclear Physics in the Office of Science of the Department of Energy, the National Science Foundation, Abilene Christian University Research Council, Research Foundation of SUNY, and Dean of the College of Arts and Sciences, Vanderbilt University (U.S.A), Ministry of Education, Culture, Sports, Science, and Technology and the Japan Society for the Promotion of Science (Japan), Conselho Nacional de Desenvolvimento Científico e Tecnológico and Fundação de Amparo à Pesquisa do Estado de São Paulo (Brazil), Natural Science Foundation of China (P. R. China), Ministry of Education, Youth and Sports (Czech Republic), Centre National de la Recherche Scientifique, Commissariat à l'Énergie Atomique, and Institut National de Physique Nucléaire et de Physique des Particules (France), Bundesministerium für Bildung und Forschung, Deutscher Akademischer Austausch Dienst, and Alexander von Humboldt Stiftung (Germany), Hungarian National Science Fund, OTKA (Hungary), Department of Atomic Energy and Department of Science and Technology (India), Israel Science Foundation (Israel), National Research Foundation and WCU program of the Ministry of Education Science and Technology (Korea), Ministry of Education and Science, Russian Academy of Sciences, Federal Agency of Atomic Energy (Russia), VR and Wallenberg Foundation (Sweden), the U.S. Civilian Research and Development Foundation for the Independent States of the Former Soviet Union, the US-Hungarian Fulbright Foundation for Educational Exchange, and the US-Israel Binational Science Foundation.

* Deceased

† PHENIX Co-Spokesperson: morrison@bnl.gov

‡ PHENIX Co-Spokesperson: jamie.nagle@colorado.edu

- [1] V. Khachatryan et al. (CMS Collaboration), *JHEP* **1009**, 091 (2010).
- [2] B. Abelev et al. (STAR Collaboration), *Phys. Rev. C* **80**, 064912 (2009).
- [3] B. Alver et al. (PHOBOS Collaboration), *Phys. Rev. Lett.* **104**, 062301 (2010).
- [4] A. Dumitru, K. Dusling, F. Gelis, J. Jalilian-Marian, T. Lappi, et al., *Phys. Lett. B* **697**, 21 (2011).
- [5] K. Werner, I. Karpenko, and T. Pierog, *Phys. Rev. Lett.* **106**, 122004 (2011).
- [6] K. Dusling and R. Venugopalan, *Phys. Rev. Lett.* **108**, 262001 (2012).
- [7] S. Chatrchyan et al. (CMS Collaboration), *Phys. Lett. B* **718**, 795 (2013).
- [8] B. Abelev et al. (ALICE Collaboration), arXiv:1212.2001 (2012).
- [9] G. Aad et al. (ATLAS Collaboration), arXiv:1212.5198 (2012).
- [10] P. Huovinen and P. Ruuskanen, *Ann. Rev. Nucl. Part. Sci.* **56**, 163 (2006).
- [11] L. McLerran, arXiv:0807.4095 (2008).
- [12] K. Dusling and R. Venugopalan, arXiv:1211.3701 (2012).
- [13] K. Dusling and R. Venugopalan, arXiv:1302.7018 (2013).
- [14] P. Bozek, *Phys. Rev. C* **85**, 014911 (2012).
- [15] E. Shuryak and I. Zahed, arXiv:1301.4470 (2013).
- [16] M. G. Ryskin, A. D. Martin, and V. A. Khoze, *J. Phys. G: Nucl. Part. Phys.* **38**, 085006 (2011).
- [17] E. Avsar, C. Flensburg, Y. Hatta, J.-Y. Ollitrault, and T. Ueda, *Phys. Lett. B* **702**, 394 (2011).
- [18] A. Adare et al. (PHENIX Collaboration), *Phys. Rev. Lett.* **107**, 172301 (2011).
- [19] S. Adler et al. (PHENIX Collaboration), *Phys. Rev. C* **73**, 054903 (2006).
- [20] S. Adler et al. (PHENIX Collaboration), *Phys. Rev. Lett.* **96**, 222301 (2006).
- [21] B. Alver, M. Baker, C. Loizides, and P. Steinberg, arXiv:0805.4411 (2008).
- [22] A. Adare et al. (PHENIX Collaboration), arXiv:1204.0777 (2012), *Phys. Rev. C* in proof stage.
- [23] N. Ajitanand, J. Alexander, P. Chung, W. Holzmann, M. Issah, et al., *Phys. Rev. C* **72**, 011902 (2005).
- [24] C. Adler et al. (STAR Collaboration), *Phys. Rev. Lett.* **90**, 082302 (2003).
- [25] P. Bozek, private communication.
- [26] M. Luzum, *Phys. Lett. B* **696**, 499 (2011).
- [27] B. H. Alver, C. Gombeaud, M. Luzum, and J.-Y. Ollitrault, *Phys. Rev. C* **82**, 034913 (2010).
- [28] K. Aamodt et al. (ALICE Collaboration), *Phys. Lett. B* **708**, 249 (2012).
- [29] M. Gyulassy and X.-N. Wang, *Comput. Phys. Commun.* **83**, 307 (1994).
- [30] S. Adler et al., *Phys. Rev. C* **71**, 034908 (2005).
- [31] A. Adare et al. (PHENIX Collaboration), *Phys. Rev. Lett.* **105**, 062301 (2010).
- [32] R. A. Lacey, A. Taranenko, R. Wei, N. Ajitanand, J. Alexander, et al., *Phys. Rev. C* **82**, 034910 (2010).
- [33] S. Chatrchyan et al. (CMS Collaboration), *Phys. Rev. C* **87**, 014902 (2013).
- [34] S. Chatrchyan et al. (CMS Collaboration), *JHEP* **1108**, 141 (2011).